NASA TECHNICAL MEMORANDUM

NASA TM X-2804

NASA TM X-2804

SUPERSONIC AERODYNAMIC CHARACTERISTICS OF THE NORTH AMERICAN ROCKWELL ATP SHUTTLE ORBITER

by George M. Ware, Bernard Spencer, Jr., and Roger H. Fournier

Langley Research Center
Hampton, Va. 23665

NATIONAL AERONAUTICS AND SPACE ADMINISTRATION • WASHINGTON, D. C. • AUGUST 1973

1. Report No.	2. Government Accession No.	3. Recipient's Catalog No.
NASA TM X-2804		

4. Title and Subtitle	5. Report Date
SUPERSONIC AERODYNAMIC CHARACTERISTICS OF THE NORTH AMERICAN ROCKWELL ATP SHUTTLE ORBITER	August 1973
	6. Performing Organization Code
7. Author(s)	8. Performing Organization Report No.
George M. Ware, Bernard Spencer, Jr., and Roger H. Fournier	L-8840
	10. Work Unit No.
9. Performing Organization Name and Address	502-37-01-01
NASA Langley Research Center Hampton, Va. 23665	11. Contract or Grant No.
	13. Type of Report and Period Covered
12. Sponsoring Agency Name and Address	Technical Memorandum
National Aeronautics and Space Administration Washington, D.C. 20546	14. Sponsoring Agency Code

15. Supplementary Notes

16. Abstract

An investigation has been made in the Langley Unitary Plan wind tunnel to determine the supersonic aerodynamic characteristics of a 0.01925-scale model of the North American Rockwell ATP (authority-to-proceed) space shuttle orbiter configuration. The model consisted of a low-fineness-ratio body with a blended 50° swept delta wing forming an ogee planform and a center-line-mounted vertical tail. Tests were made at Mach numbers from 1.90 to 4.63, at angles of attack from -6° to 30°, at angles of sideslip of 0° and 3°, and at a Reynolds number, based on body length, of 5.3×10^6.

17. Key Words (Suggested by Author(s))	18. Distribution Statement
Space shuttle Supersonic aerodynamics Reentry	Unclassified – Unlimited

19. Security Classif. (of this report)	20. Security Classif. (of this page)	21. No. of Pages	22. Price*
Unclassified	Unclassified	33	$3.00

*For sale by the National Technical Information Service, Springfield, Virginia 22151

SUPERSONIC AERODYNAMIC CHARACTERISTICS OF THE NORTH AMERICAN ROCKWELL ATP SHUTTLE ORBITER

By George M. Ware, Bernard Spencer, Jr.,
and Roger H. Fournier
Langley Research Center

SUMMARY

An investigation has been made in the Langley Unitary Plan wind tunnel to determine the supersonic aerodynamic characteristics of a 0.01925-scale model of the North American Rockwell ATP (authority-to-proceed) space shuttle orbiter configuration. The model consisted of a low-fineness-ratio body with a blended 50° swept delta wing forming an ogee planform and a center-line-mounted vertical tail with rudder flare of 40°. Tests were made at Mach numbers from 1.90 to 4.63, at angles of attack from -6° to 30°, at angles of sideslip of 0° and 3°, and at a Reynolds number, based on body length, of 5.3×10^{6}.

The model was longitudinally stable about the center of gravity (0.65 body length for the present investigation) and could be trimmed at angles of attack encompassing those of a nominal high-cross-range (1100 nautical miles) shuttle mission. At the mission angles of attack, the trimmed lift-drag ratio was constant at about 1.75 across the Mach range from 1.90 to 4.63.

Although a rudder flare of 40° (deflecting each side of the rudder outward 20°) was incorporated primarily to improve directional stability, the relatively high drag of this tail configuration acting above the vehicle center of gravity resulted in a favorable trim shift in pitch.

The directional stability decreased with increasing Mach number and angle of attack. The model was directionally unstable at angles of attack above 16° at a Mach number of 1.90 and above 12° at a Mach number of 4.63. The dynamic directional stability parameter $C_{n_{\beta_{dyn}}}$, however, was positive for all test conditions.

INTRODUCTION

During the past several years, the National Aeronautics and Space Administration and the aerospace industry have performed in-depth analytical and experimental studies

leading to the development of an efficient and cost-effective transportation system capable of transferring large payloads from earth to earth orbit and return. (See, for example, ref. 1.) The system as presently configured (fig. 1) consists of a delta-wing orbiter, a large external fuel tank, and a pair of strap-on solid rocket boosters. The fuel tank and rocket boosters are jettisoned during the mission and the orbiter returns to earth as an independent element. The orbiter enters the atmosphere at high angles of attack (30° to 45°) and as Mach number and altitude decrease, pitches down to maximum lift-drag ratio attitudes to attain maximum cross range. Final recovery is accomplished with an unpowered approach and horizontal landing.

The purpose of the present investigation was to determine the basic supersonic longitudinal and lateral-directional aerodynamic characteristics of a 0.01925-scale model of the North American Rockwell orbiter concept designated as the ATP (authority-to-proceed) configuration. The tests were conducted in the Langley Unitary Plan wind tunnel at Mach numbers from 1.90 to 4.63, at angles of attack from -6° to 30°, at angles of sideslip of 0° and 3°, and at a Reynolds number, based on body length, of 5.3×10^6. A complete listing of the basic data is given in reference 2.

SYMBOLS

The longitudinal data are referred to the stability-axis system, and the lateral-directional data are referred to the body-axis system. All coefficients are normalized with respect to the area of the basic 50° swept delta wing excluding the wing-body fairing (fig. 2), the length of mean aerodynamic chord of the 50° swept delta wing, or the total wing span. The moment reference point corresponds to a center-of-gravity location at 0.65 body length.

b reference span (maximum wing span), 49.27 cm (19.40 in.)

$\bar{c}$ mean aerodynamic chord of 50° delta wing, 25.42 cm (10.01 in.)

C_D drag coefficient, $\frac{\text{Drag}}{q_\infty S}$

C_L lift coefficient, $\frac{\text{Lift}}{q_\infty S}$

$C_{L_\alpha} = \frac{\partial C_L}{\partial \alpha}$

C_l rolling-moment coefficient, $\frac{\text{Rolling moment}}{q_\infty S b}$

$C_{l_\beta} = \frac{\Delta C_l}{\Delta \beta}$ per degree at $\beta = 0^o$ and 3^o

C_m pitching-moment coefficient, $\frac{\text{Pitching moment}}{q_\infty S \bar{c}}$

$C_{m,o}$ pitching-moment coefficient at zero lift

$C_{m_\alpha} = \frac{\partial C_m}{\partial \alpha}$

C_n yawing-moment coefficient, $\frac{\text{Yawing moment}}{q_\infty S b}$

$C_{n_\beta} = \frac{\Delta C_n}{\Delta \beta}$ per degree at $\beta = 0^o$ and 3^o

$C_{n_{\beta_{dyn}}} = C_{n_\beta} \cos \alpha - C_{l_\beta} \frac{I_Z}{I_X} \sin \alpha$

C_p pressure coefficient

C_Y side-force coefficient, $\frac{\text{Side force}}{q_\infty S}$

$C_{Y_\beta} = \frac{\Delta C_Y}{\Delta \beta}$ per degree at $\beta = 0^o$ and 3^o

$\frac{I_Z}{I_X}$ ratio of moments of inertia about yaw (Z) and roll (X) body axes, 8.0 (design value obtained from contractor)

L/D lift-drag ratio

l length of body, m

M Mach number

q_∞ dynamic pressure, N/m^2

S area of 50^o delta wing, 0.111 m^2 (1.193 ft^2)

α angle of attack, deg

β angle of sideslip, deg

δ_e elevon deflection angle (positive when trailing edge is deflected downward), deg

Subscripts:

dyn	dynamic
in	inboard
max	maximum
min	minimum
out	outboard

DESCRIPTION OF MODEL

Sketches and photographs of the 0.01925-scale model used in the investigation are presented in figures 2 and 3, respectively. The model had a 50° swept delta wing that was blended into the body forming an ogee planform. The wing geometry and other pertinent details are given in table I. For all tail-on tests, the vertical tail had a rudder flare of 40°, obtained by deflecting each side of the rudder 20° outward. With this setting, the configuration is considered to be the supersonic configuration.

Large fairings on each side at the base of the model represented the housing of the orbital maneuvering system (OMS) for the vehicle, and a fairing extending from the canopy aft to the vertical tail along the top of the body simulated the housing for the cargo handling arms. The elevons were split into two spanwise segments and could be deflected individually or as a unit.

APPARATUS, TESTS, AND CORRECTIONS

Tests were conducted in both the low and high Mach number test sections of the Langley Unitary Plan wind tunnel, which is a variable-pressure continuous-flow tunnel. The test sections are approximately 1.22 meters (4 feet) square and 2.13 meters (7 feet) long. The nozzles leading to the test sections are of the asymmetric sliding-block type, which permit a continuous variation in Mach number from about 1.40 to 2.90 in the low Mach number test section and from about 2.30 to 4.70 in the high Mach number test section. The Mach number, stagnation temperatures, stagnation pressures, and Reynolds numbers were as follows:

Mach number	Stagnation temperature		Stagnation pressure		Reynolds number	
	K	^{o}F	kN/m^2	lb/ft^2	Per meter	Per foot
1.90	339	150	76.08	1589	8.20×10^6	2.5×10^6
2.36	339	150	94.56	1975	↓	↓
2.86	339	150	123.05	2570		
3.96	352	175	231.21	4829		
4.63	352	175	315.72	6594		

The stagnation dewpoint was maintained below 239 K (-30^{o} F) to insure negligible condensation effects. To insure turbulent flow over the model, a 0.16-cm-wide (1/16-inch) strip of No. 60 grit was affixed 3.05 cm (1.2 inches) aft of the apex of the model nose and 1.02 cm (0.4 inch) aft of the leading edge of the wing and vertical tail measured in the streamwise direction.

Tests were made over an angle-of-attack range from about -6^{o} to 30^{o} for angles of sideslip of 0^{o} and 3^{o} at a constant Reynolds number of 5.3×10^6, based on body length. The model was sting supported and forces and moments were measured by an internal strain-gage balance. The balance and sting were calibrated for the effects of bending under load in both the longitudinal and lateral planes and the angle of attack was corrected for flow misalinement. The drag values presented herein are the gross drag values which include base drag. Balance chamber pressure, body base pressure, and OMS housing base pressure were measured, however, and are presented as figure 4 for the model with undeflected controls at each test Mach number.

RESULTS AND DISCUSSION

Flight Regimes

The return-from-orbit flight plan may call for entry into the earth's atmosphere at high angles of attack near $C_{L_{max}}$ in a semiballistic mode for low-cross-range missions and at moderate angles of attack ($\alpha \approx 30^{o}$) for high-cross-range missions. An attitude control propulsion system (ACPS) is used for pitch, yaw, and roll control during the high-altitude hypersonic flight where dynamic pressures are low. At lower altitudes when dynamic pressures become sufficiently high, a mixed-mode control is possible (that is, both aerodynamic and ACPS control systems). In the supersonic and transonic phase of the flight the vehicle is in a transition maneuver from high to low angles of attack where aerodynamic controls alone are to be used. At subsonic speeds, an aircraft-like glide flight to a horizontal landing is made. A nominal angle-of-attack schedule for a

high-cross-range (1100 nautical miles) mission is presented in figure 5. The angle of attack of the orbiter in the speed range of the present investigation (M = 1.90 to 4.63) varies from about 23° to 11°. Although vehicle angles of attack at supersonic speeds may be as high as 45° for other missions such as a minimum-cross-range quick-return-to-earth flight, the α schedule of figure 5 is considered as representative of a nominal mission for the vehicle of the present investigation.

Longitudinal Aerodynamic Characteristics

The basic longitudinal aerodynamic characteristics of the model with all controls neutral are presented across the test Mach number range in figure 6. The variation of lift with angle of attack was reasonably linear for Mach numbers from 1.90 to 2.86. At the higher Mach numbers, however, rather large increases in the variation of lift with angle of attack are noted; these values are typical of high supersonic and hypersonic characteristics. The configuration was longitudinally stable at all Mach numbers for the center of gravity of the present investigation (0.65ℓ). The low angle-of-attack characteristics (through $\alpha = 0^{\circ}$) and the maximum untrimmed lift-drag values from figure 6 are summarized in figure 7. These data show that there was the usual decrease in longitudinal stability and low-angle lift-curve slope with Mach number. The maximum untrimmed lift-drag value was about 2.1 and remained approximately the same across the Mach range.

The pitching moment at zero lift $C_{m,o}$ decreased with increasing Mach number but had positive values for $M \leq 2.5$. Large nose-down $C_{m,o}$ is noted for the body alone (tail off). (See fig. 8.) This negative $C_{m,o}$ is belived to arise from a combination of forebody positive camber and possible shock interference in the canopy region as illustrated in the schlieren photographs of figure 9. The favorable positive shift in $C_{m,o}$ was a result of the drag of the vertical tail with 40° rudder flare acting above the center of gravity. (See fig. 8.) Although rudder flare was incorporated primarily to improve directional stability, the high drag of this tail configuration is favorable in pitch, especially at the lower angles of attack and Mach numbers.

The effect of elevon deflection is shown in figure 10. Deflecting only the inboard elevons (figs. 10(d) and 10(e)), which had about the same area as the outboard elevons, proved to be less than half as effective as deflecting the total elevon. Because rather high trim angles of attack are required for the mission, it appears that full-span elevons will be necessary. The trim characteristics of figure 10 are summarized in figure 11. Extrapolation of these data to include the trim α required for the orbiter angle of attack—Mach number schedule (fig. 5) has been accomplished by using as a guide the elevon effects on C_m, C_L, and C_D from an earlier orbiter concept (ref. 3) and recent unpublished results obtained on a similar configuration tested to an angle of attack of

approximately 50°. The data of figure 11 indicate that the configuration was longitudinally stable at angles of attack encompassing the α schedule although the trimmed stability level was near zero at $M = 4.63$. Trimmed $(L/D)_{max}$ was about 1.75 and was essentially constant from $M = 1.90$ to 4.63.

Lateral-Directional Stability Characteristics

The lateral-directional stability characteristics of the model are presented in figure 12. These data were obtained by taking the difference in lateral coefficients measured at angles of sideslip of 0° and 3° over the test angle-of-attack range. The angles of sideslip were selected after tests were made over a sideslip range at several angles of attack to insure that the variations of the lateral coefficients were linear. All lateral-directional data are for zero elevon deflection.

The data of figure 12 show decreasing directional stability with increasing Mach number. Large losses in directional stability with increasing angle of attack are also noted at all Mach numbers. The model became directionally unstable at $\alpha \approx 16^{\circ}$ at $M = 1.90$ and was neutrally stable from $\alpha = 0^{\circ}$ to 12° at $M = 4.63$ before becoming unstable. In general, the complete model had positive effective dihedral $\left(-C_{l_\beta}\right)$ over the Mach number range and at angles of attack above 4°.

The vertical-tail effectiveness may be seen in figures 12(a) to 12(c) for Mach numbers from 1.90 to 2.86. It should be pointed out that when the vertical tail was removed, the housing that extended along the top of the fuselage was also removed. (See fig 2.) The effect of shielding the vertical tail by the wing is shown by noting that at an angle of attack of about 25°, the value of C_{n_β} for the complete model decreases to about that of the tail-off configuration. Therefore, flaring the rudder to increase directional stability at angles of attack above 25° would be ineffective.

At high angles of attack, however, the parameter $C_{n_{\beta_{dyn}}}$ $\left(\text{where } C_{n_{\beta_{dyn}}} = C_{n_\beta} \cos\alpha - C_{l_\beta}\frac{I_Z}{I_X}\sin\alpha\right)$ has been used as a criterion for directional stability (ref. 4) in that positive values of this parameter tend to prevent aperiodic divergence. A comparison of the dynamic and static C_{n_β} parameters for the nominal flight profile across the Mach range is given in figure 13. The values of $C_{n_{\beta_{dyn}}}$ remained positive at all Mach numbers.

SUMMARY OF RESULTS

Supersonic wind-tunnel tests have been made over a Mach number range from 1.90 to 4.63 to determine the aerodynamic characteristics of a 0.01925-scale model of the

North American Rockwell ATP (authority-to-proceed) space shuttle orbiter. The results are summarized as follows:

1. The model was longitudinally stable about the center of gravity (0.65 body length for the present investigation) and could be trimmed at angles of attack encompassing those of a nominal high-cross-range (1100 nautical miles) shuttle mission. At the mission angles of attack, the trimmed lift-drag ratio was constant at about 1.75 across the Mach range from 1.90 to 4.63.

2. Although a rudder flare of 40° (deflecting each side of the rudder outward 20°) was incorporated primarily to improve directional stability, the relatively high drag of this tail configuration acting above the vehicle center of gravity resulted in a favorable trim shift in pitch.

3. The directional stability decreased with increasing Mach number and angle of attack. The model was directionally unstable at angles of attack above 16° at a Mach number of 1.90 and above 12° at a Mach number of 4.63. The dynamic directional stability parameter $C_{n_{\beta_{dyn}}}$, however, was positive for all test conditions.

Langley Research Center,
National Aeronautics and Space Administration,
Hampton, Va., May 29, 1973.

REFERENCES

1. Anon.: Alternate Space Shuttle Concepts Study. Pt. II – Technical Summary. Vol. II – Orbiter Definition. MSC-03810, B-1 (Contract NAS 9-11160), Grumman/Boeing, July 6, 1971. (Available as NASA CR-115654.)

2. Fournier, R.; and Spencer, B.: Aerodynamic Stability and Control Characteristics of a .01925 Scale Model NR ATP Orbiter at Mach Numbers From 1.9 to 4.63. DMS-DR-2001 (Contract NAS 8-4016), Space Div., Chrysler Corp., Nov. 1972. (Available as NASA CR-128750.)

3. Rainey, Robert W.; Ware, George M.; Powell, Richard W.; Brown, Lawrence W.; and Stone, David R.: Grumman H-33 Space Shuttle Orbiter Aerodynamic and Handling-Qualities Study. NASA TN D-6948, 1972.

4. Moul, Martin T.; and Paulson, John W.: Dynamic Lateral Behavior of High-Performance Aircraft. NACA RM L58E16, 1958.

TABLE I.- GEOMETRIC CHARACTERISTICS OF 0.01925-SCALE MODEL

Body:	
Overall length, cm	64.949
Maximum height, cm	11.637
Maximum width, cm	11.635
Fineness ratio	5.527
Base area, m^2	0.00644
Cavity area, m^2	0.00496
Orbital maneuvering system pod base area (total), m^2	0.00157
Wing:[a]	
Area,[b] m^2	0.111
Span,[b] cm	49.271
Aspect ratio	2.190
Dihedral angle, deg	3.500
Leading-edge sweep angle, deg	50.000
Trailing-edge sweep angle, deg	0.000
Root chord at center line, cm	37.188
Tip chord, cm	7.810
Mean aerodynamic chord,[b] cm	25.425
Airfoil section at body	------
Airfoil section at 0.34 semispan	Modified 9.48% thick 64 series
Airfoil section at 0.60 semispan	NACA 0008-64
Airfoil section at tip	NACA 0008-64
Incidence at body, deg	3.000
Incidence at tip, deg	-2.000
Vertical tail:	
Area including voids, m^2	0.014
Span, cm	15.837
Aspect ratio	1.675
Leading-edge sweep angle, deg	45.000
Trailing-edge sweep angle, deg	26.361
Root chord, cm	13.471
Tip chord, cm	5.371
Airfoil	5^o half-angle double wedge

[a]Basic 50^o wing excluding the blended wing-body juncture.

[b]Model reference dimension.

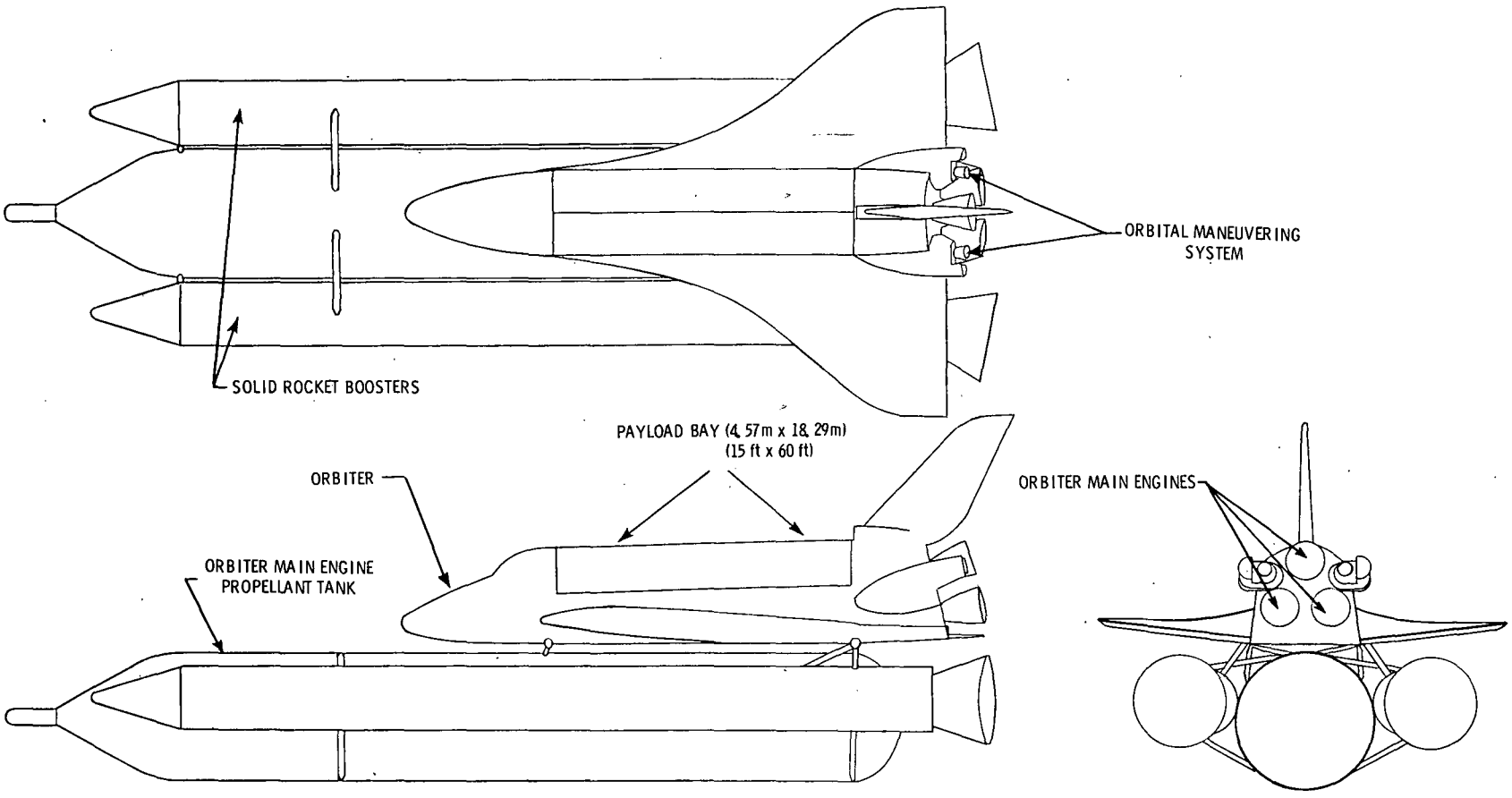

Figure 1.- General arrangement of space shuttle concept.

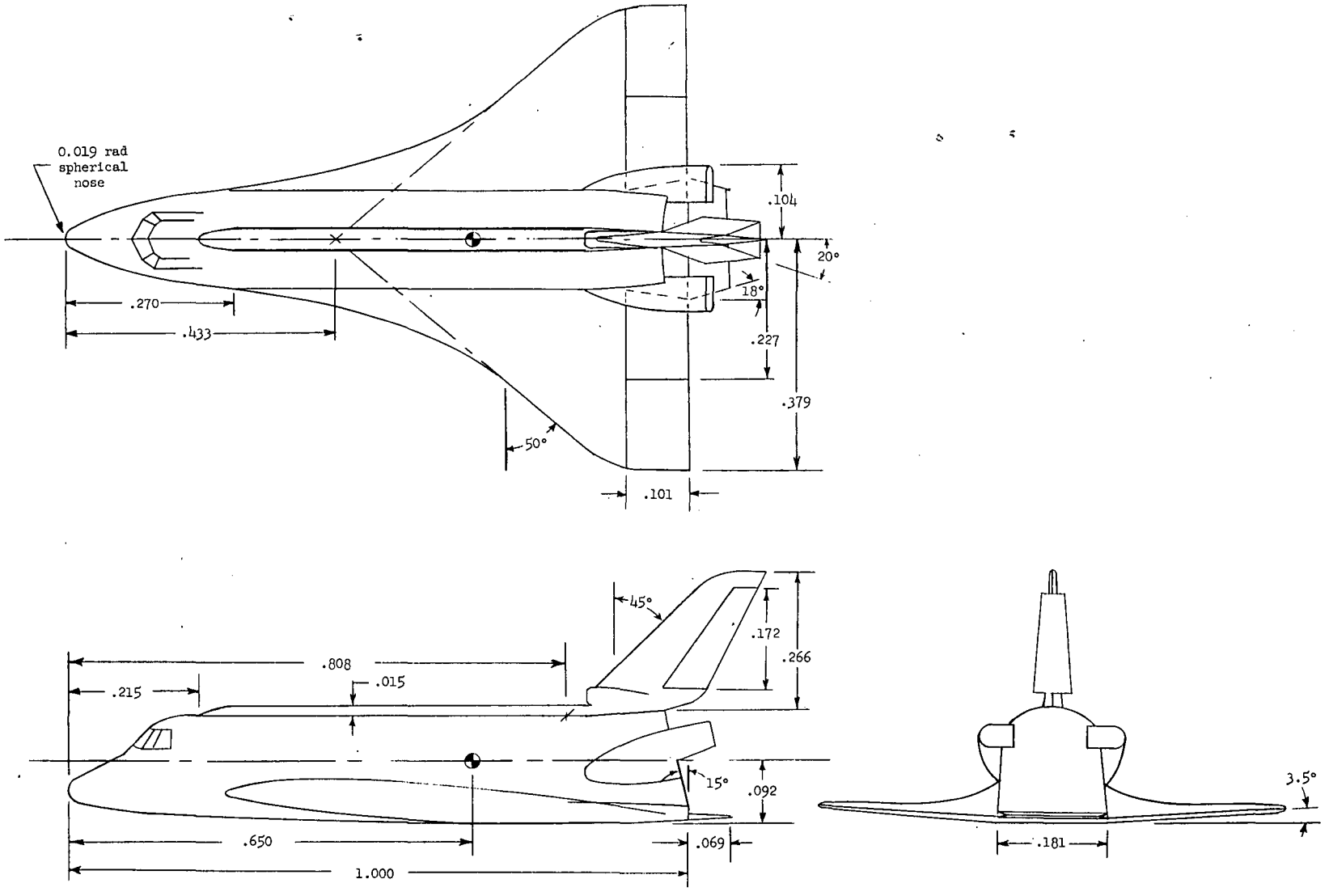

Figure 2.- Sketch of model used in investigation. All linear dimensions are in terms of body length (64.95 cm).

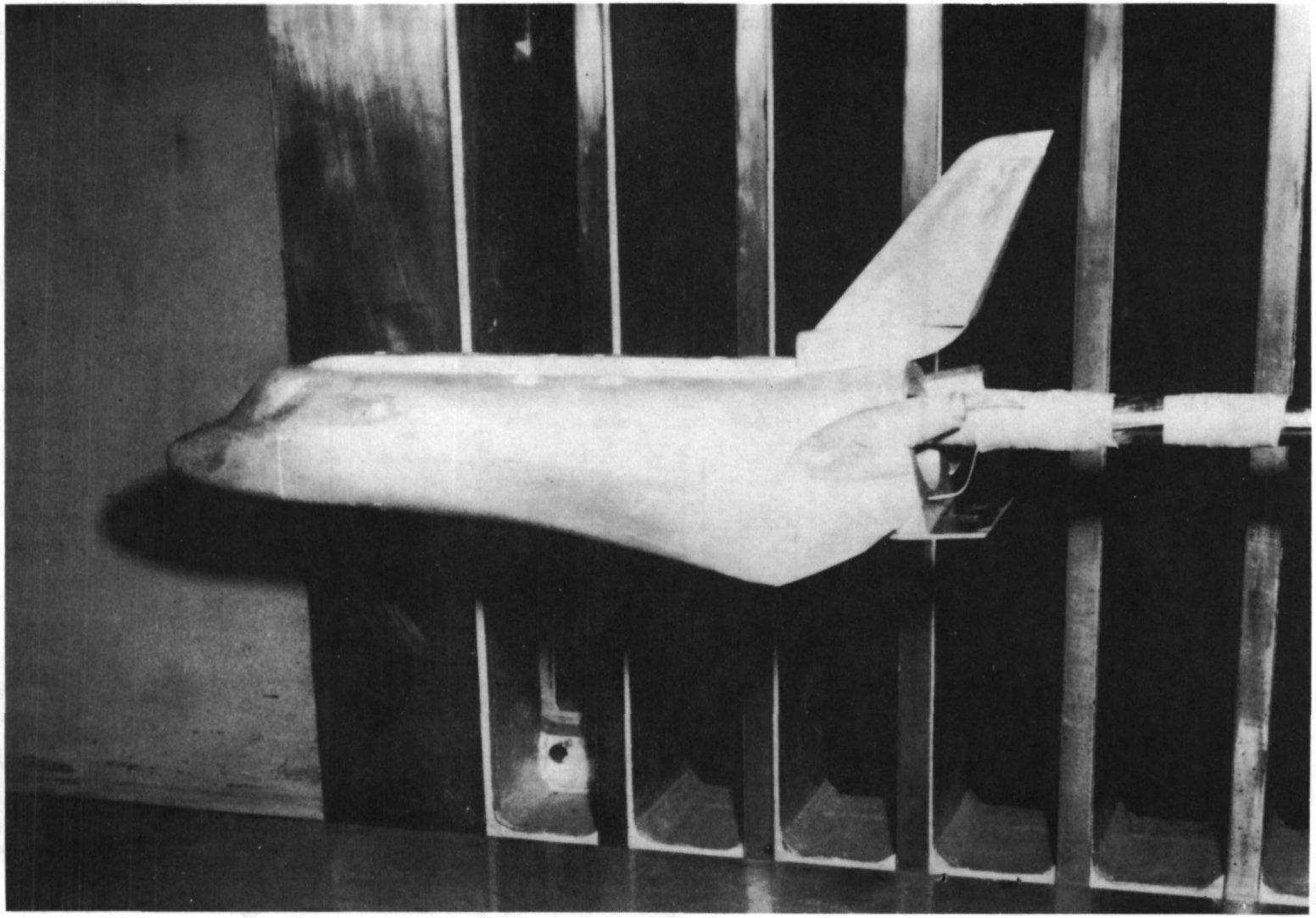

L-73-3080

Figure 3.- Photograph of model used in investigation.

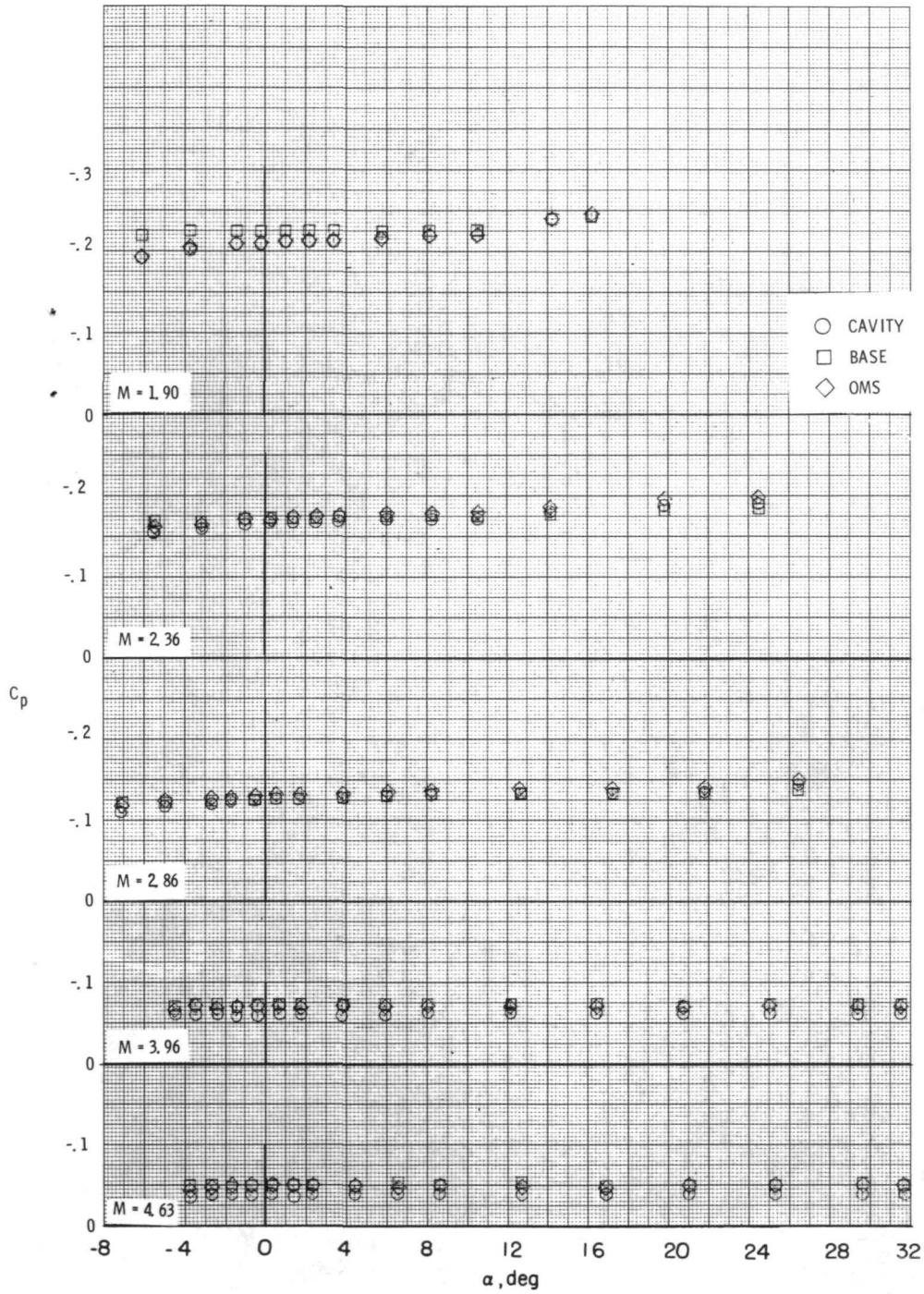

Figure 4.- Typical base pressure coefficients.

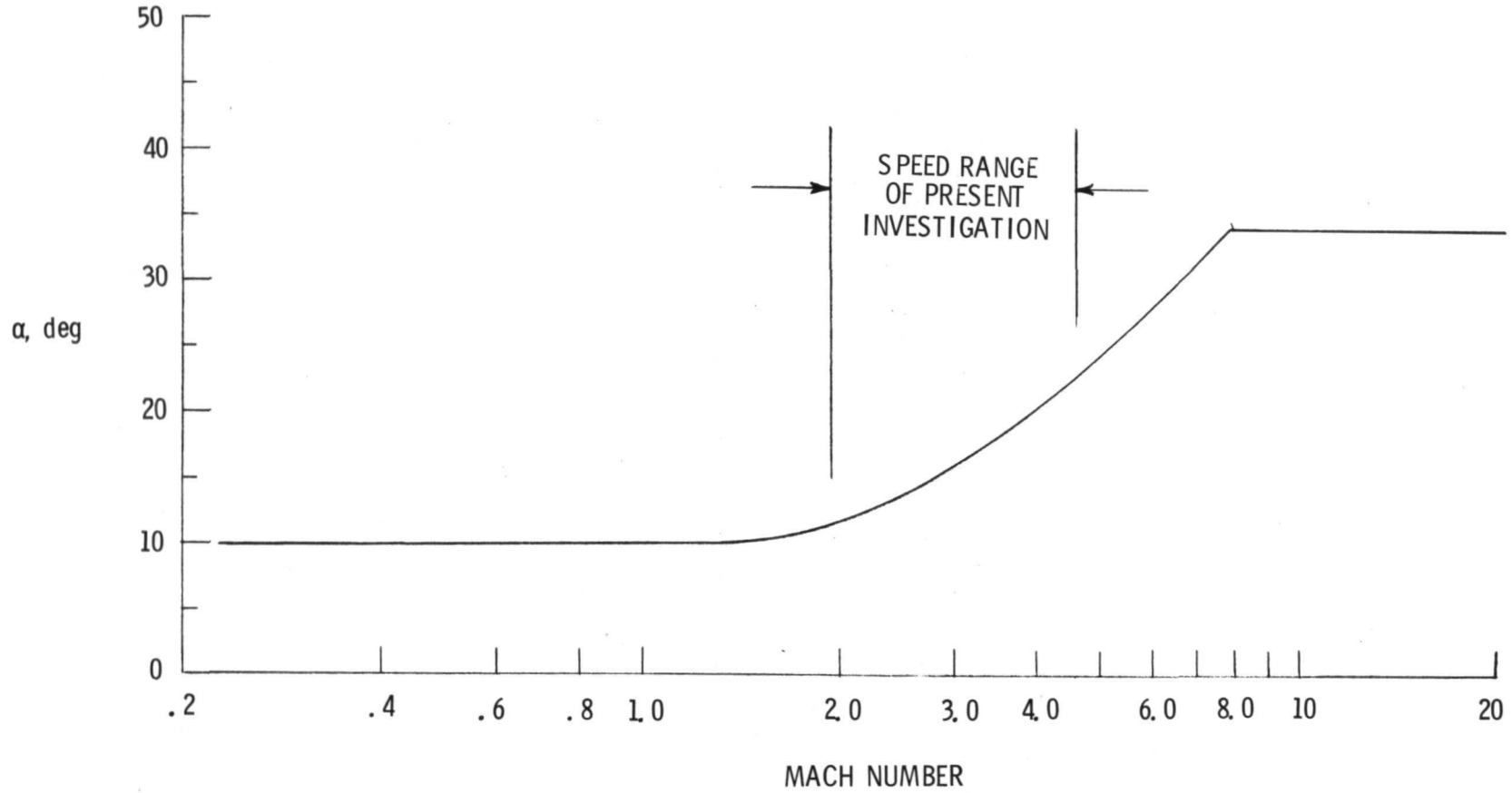

Figure 5.- Nominal operational angle-of-attack schedule for high-cross-range mission.

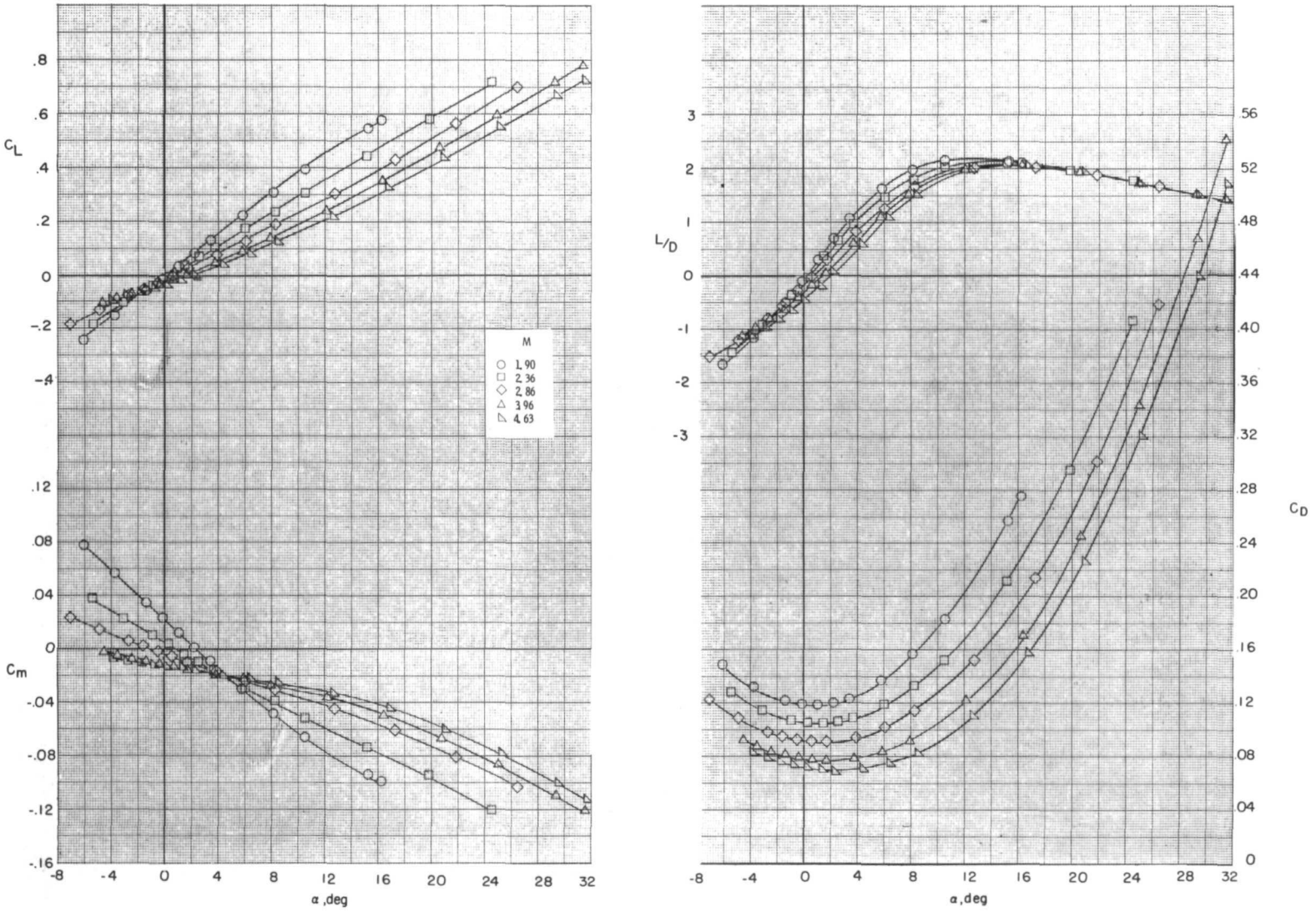

Figure 6.- Effect of Mach number on longitudinal aerodynamic characteristics of the model.

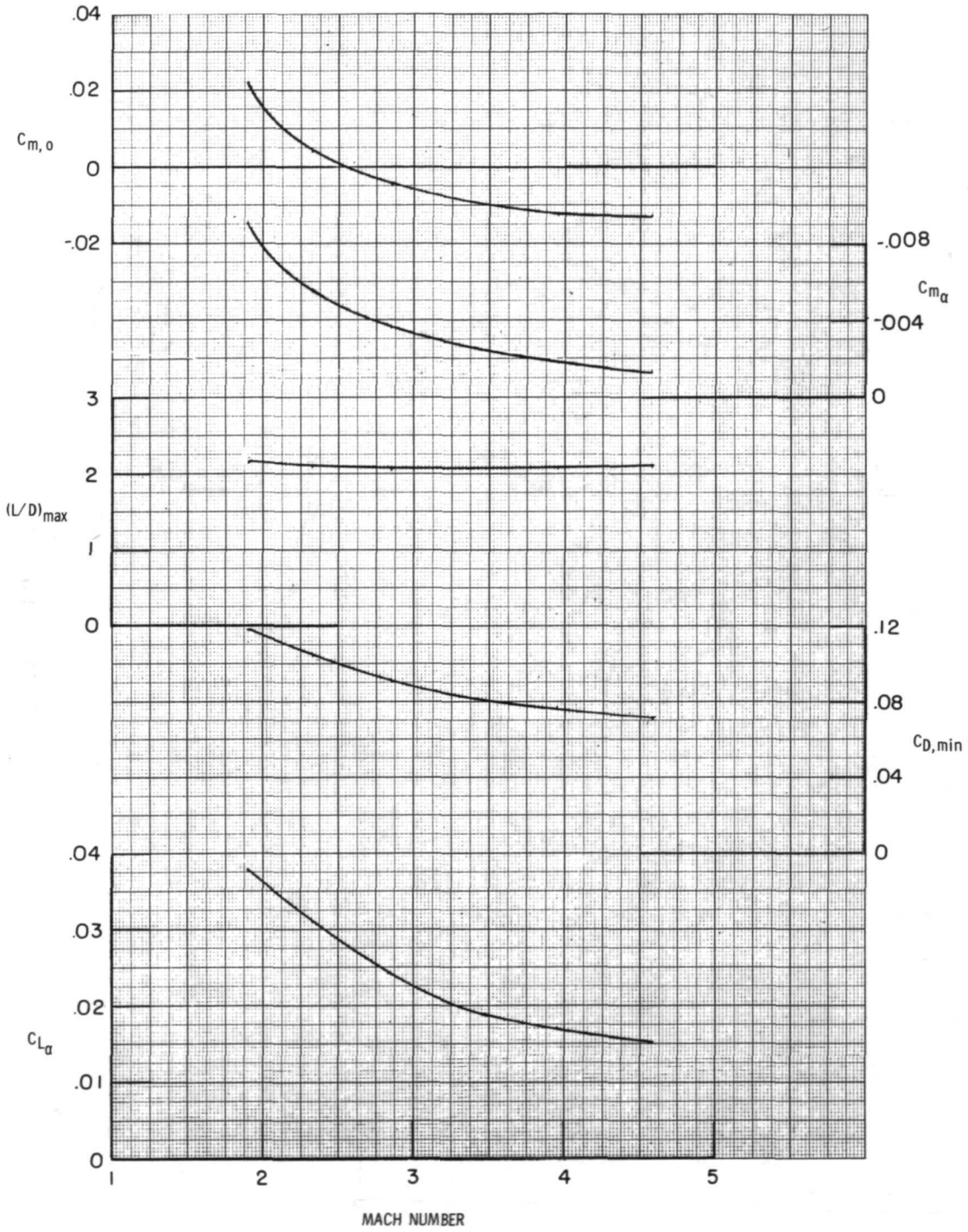

Figure 7.- Summary of untrimmed longitudinal aerodynamic characteristics.

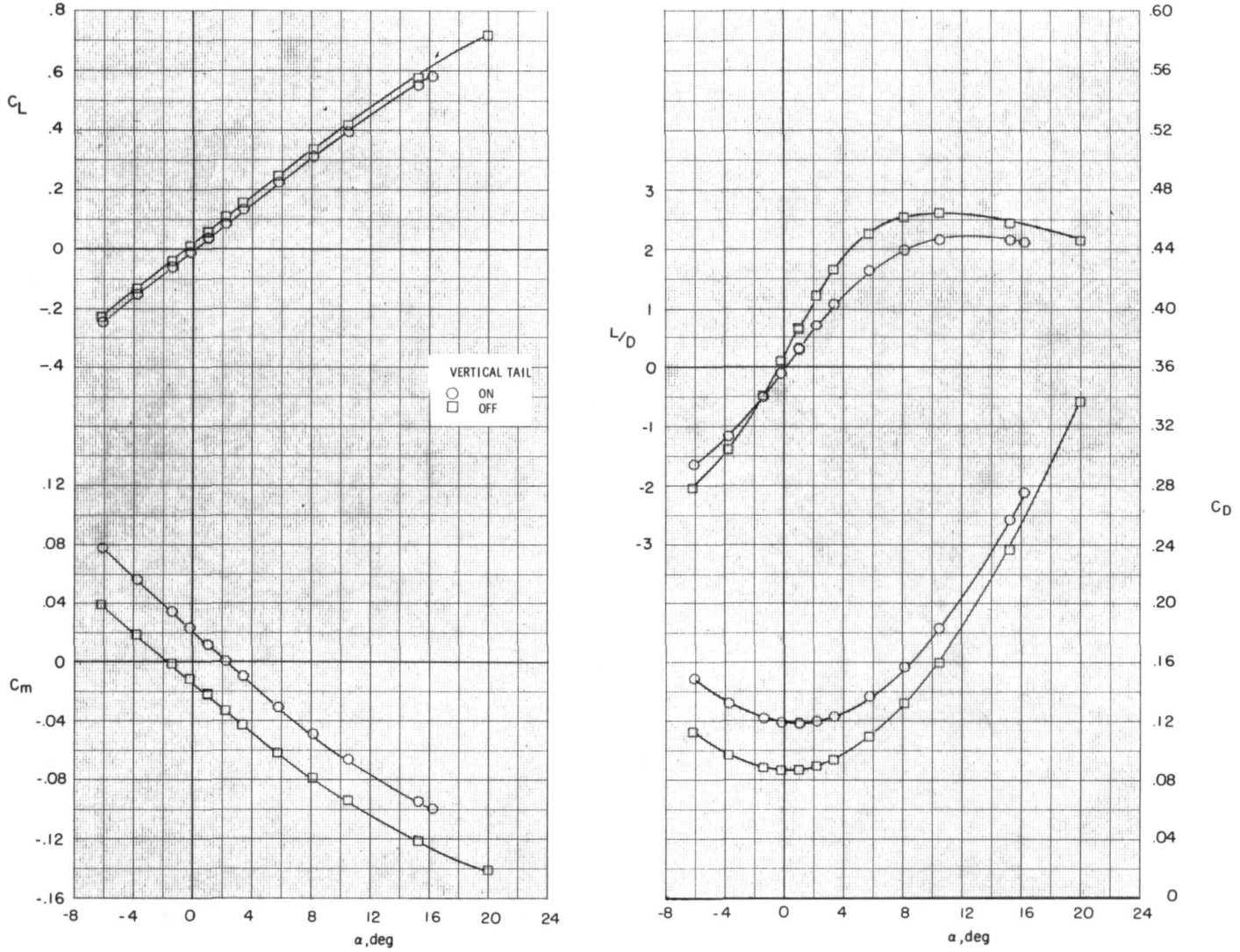

(a) M = 1.90.

Figure 8.- Effect of vertical tail on longitudinal aerodynamic characteristics of the model.

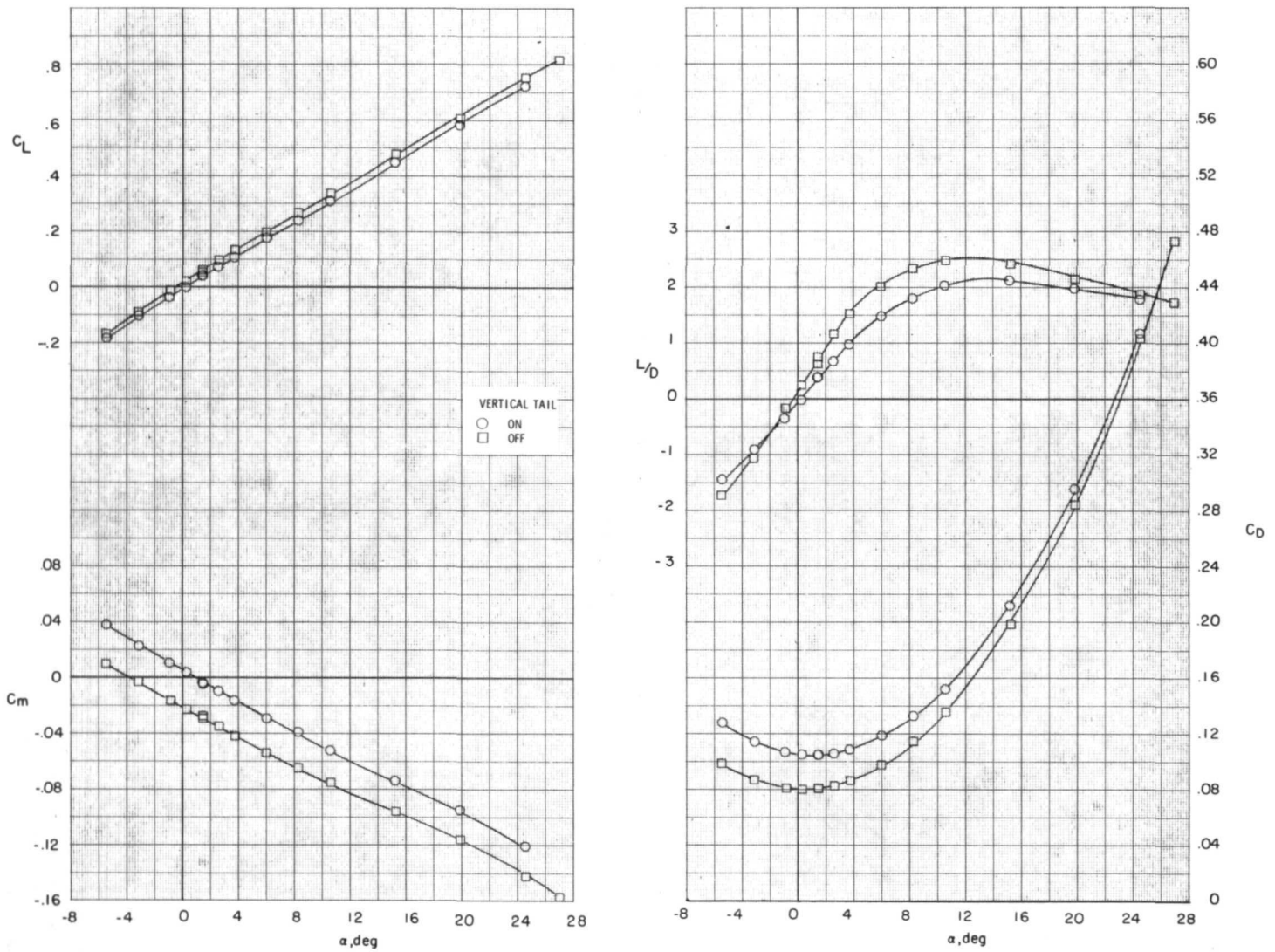

(b) M = 2.36.

Figure 8.- Continued.

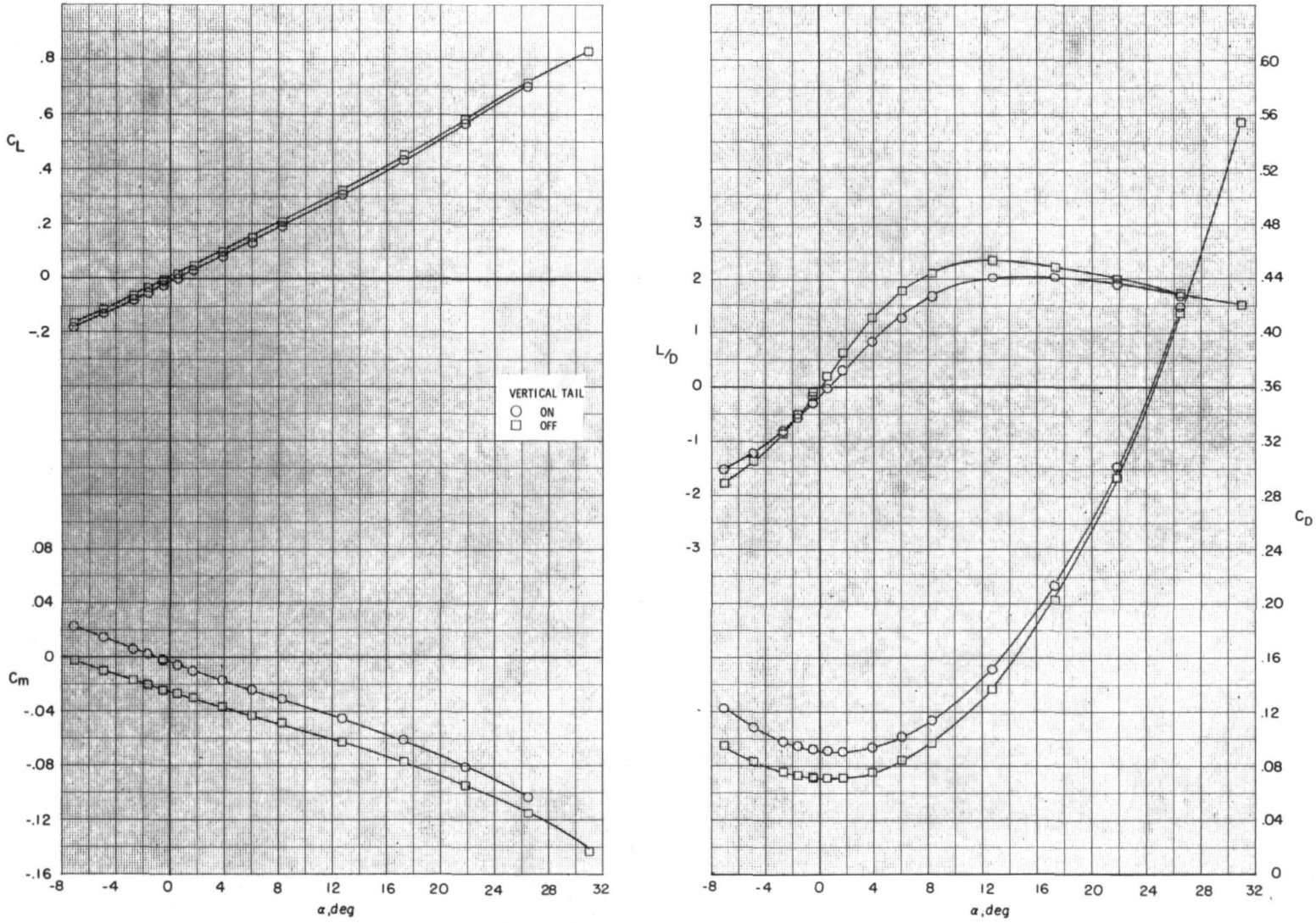

(c) M = 2.86.

Figure 8.- Concluded.

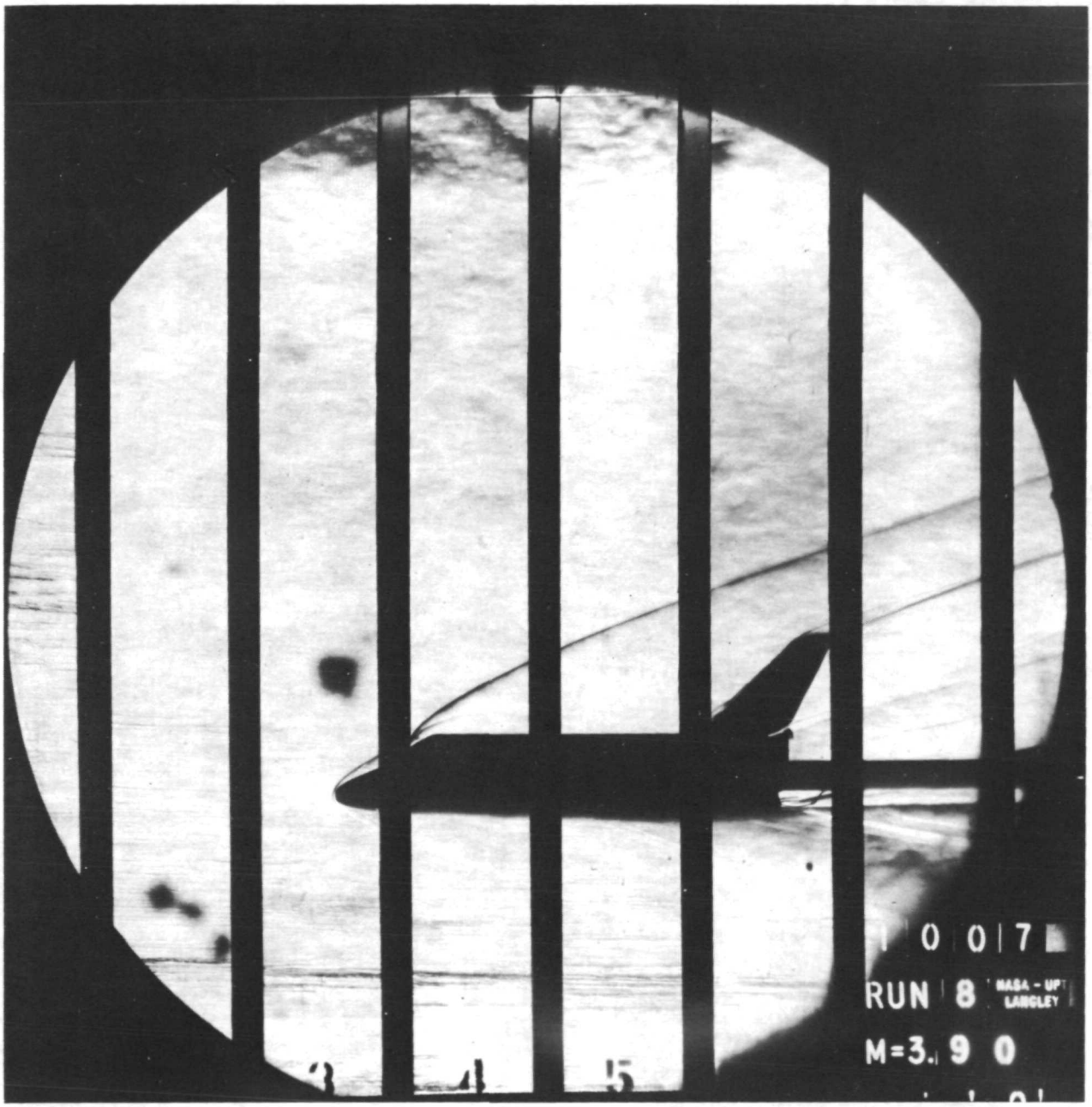

L-73-3081

Figure 9.- Schlieren photograph of model. M = 3.90; $\alpha = 0^{o}$.

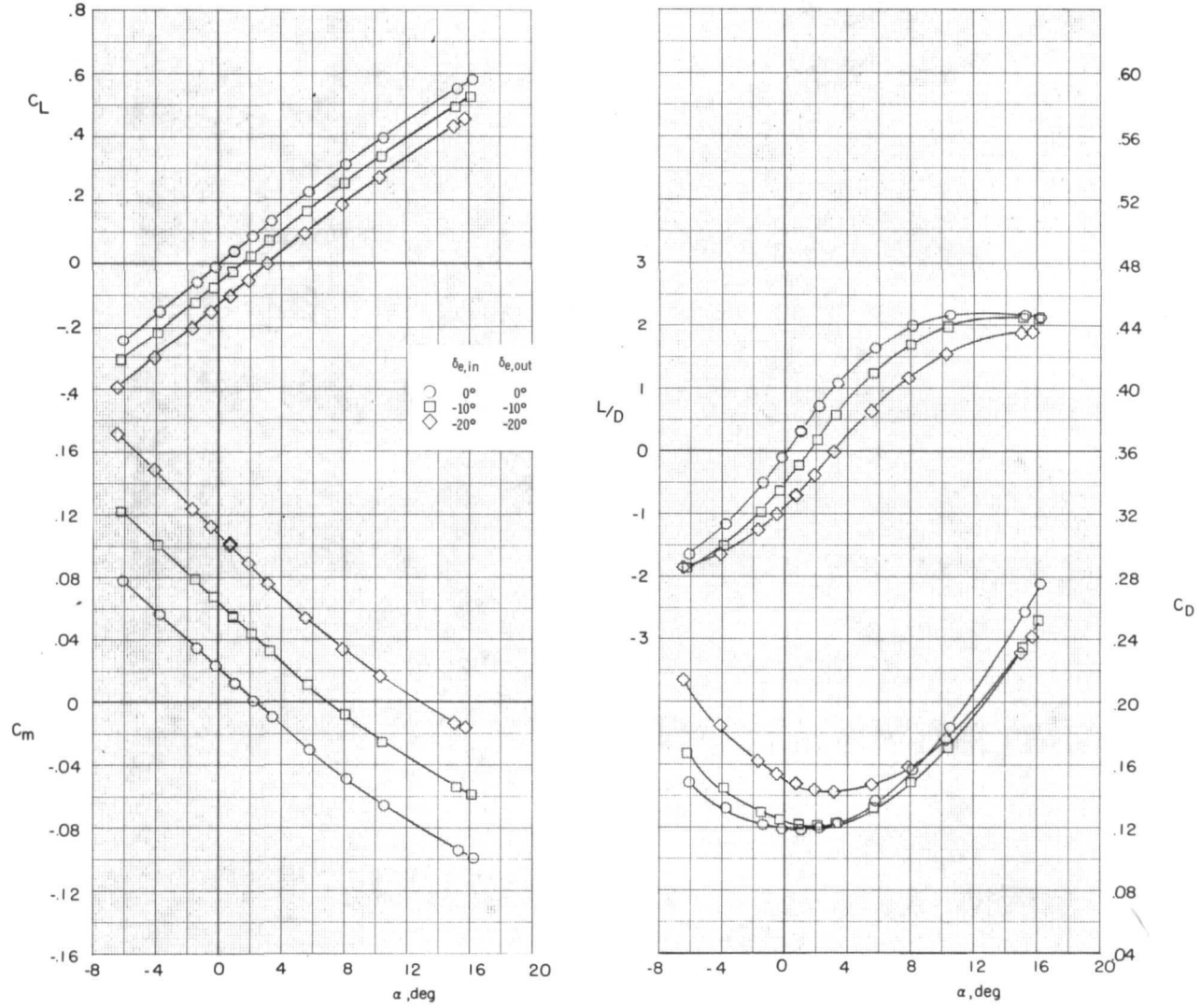

(a) M = 1.90.

Figure 10.- Effect of elevon deflection on longitudinal aerodynamic characteristics of the model.

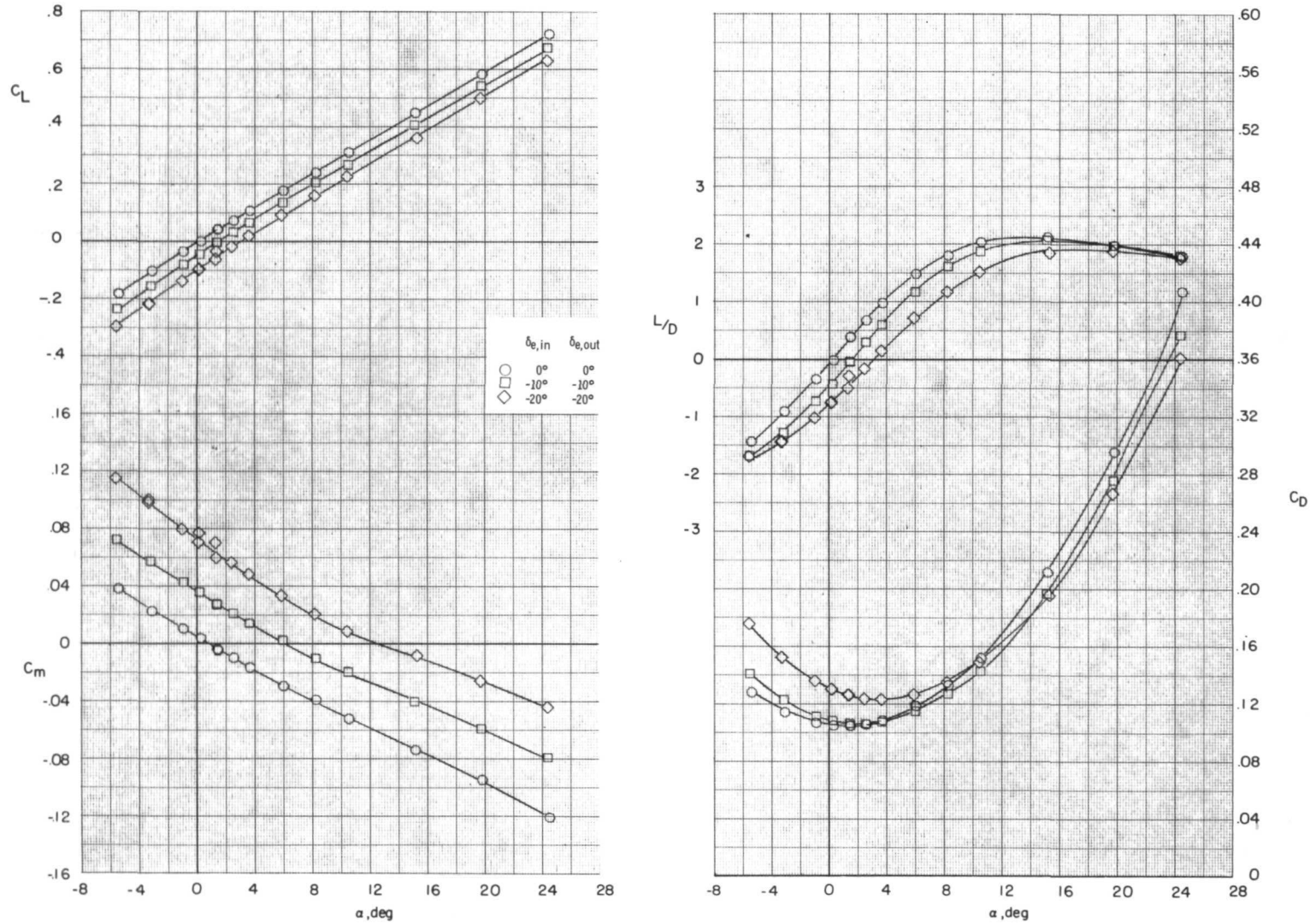

(b) M = 2.36.

Figure 10.- Continued.

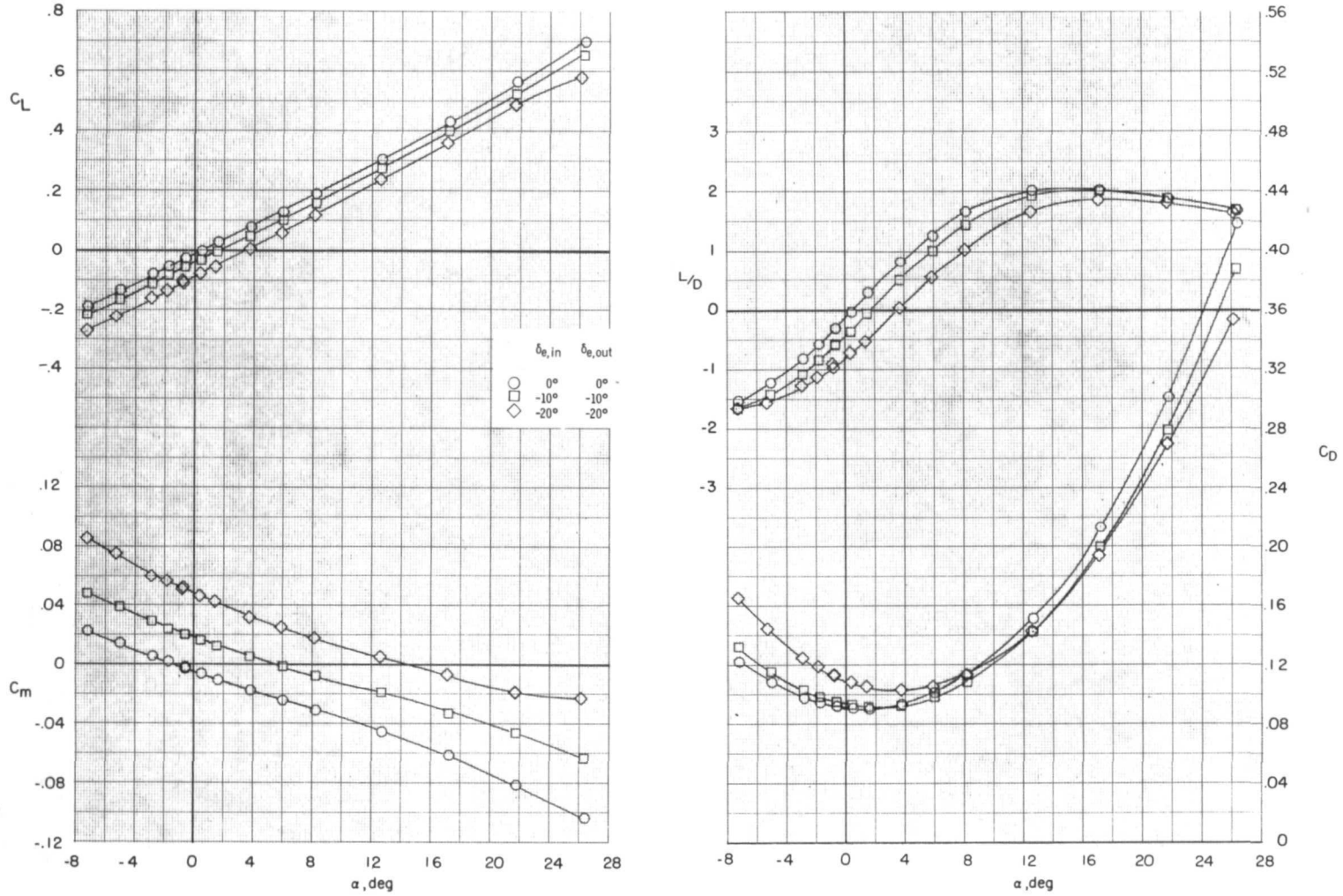

(c) M = 2.86.

Figure 10.- Continued.

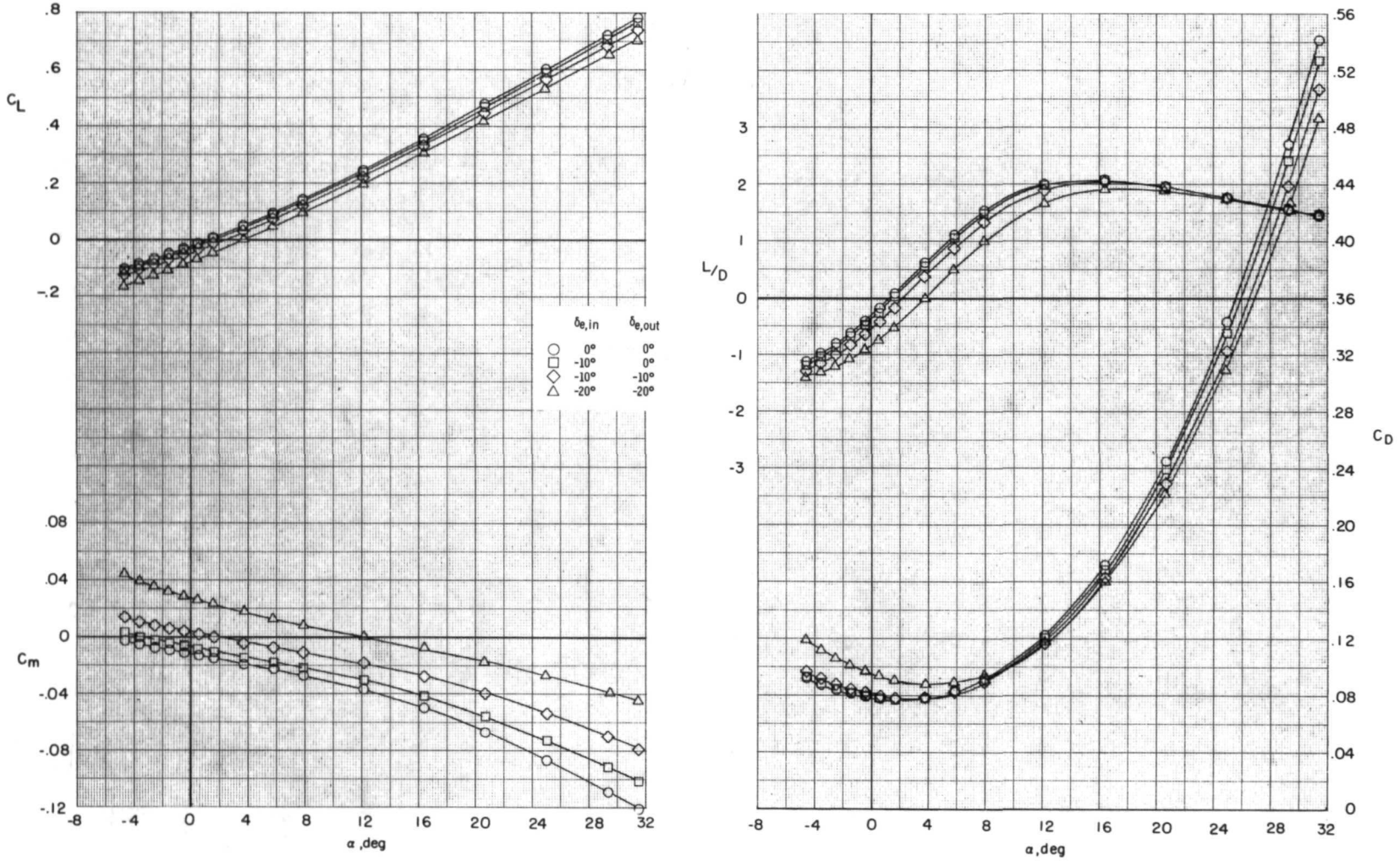

(d) M = 3.96.

Figure 10.- Continued.

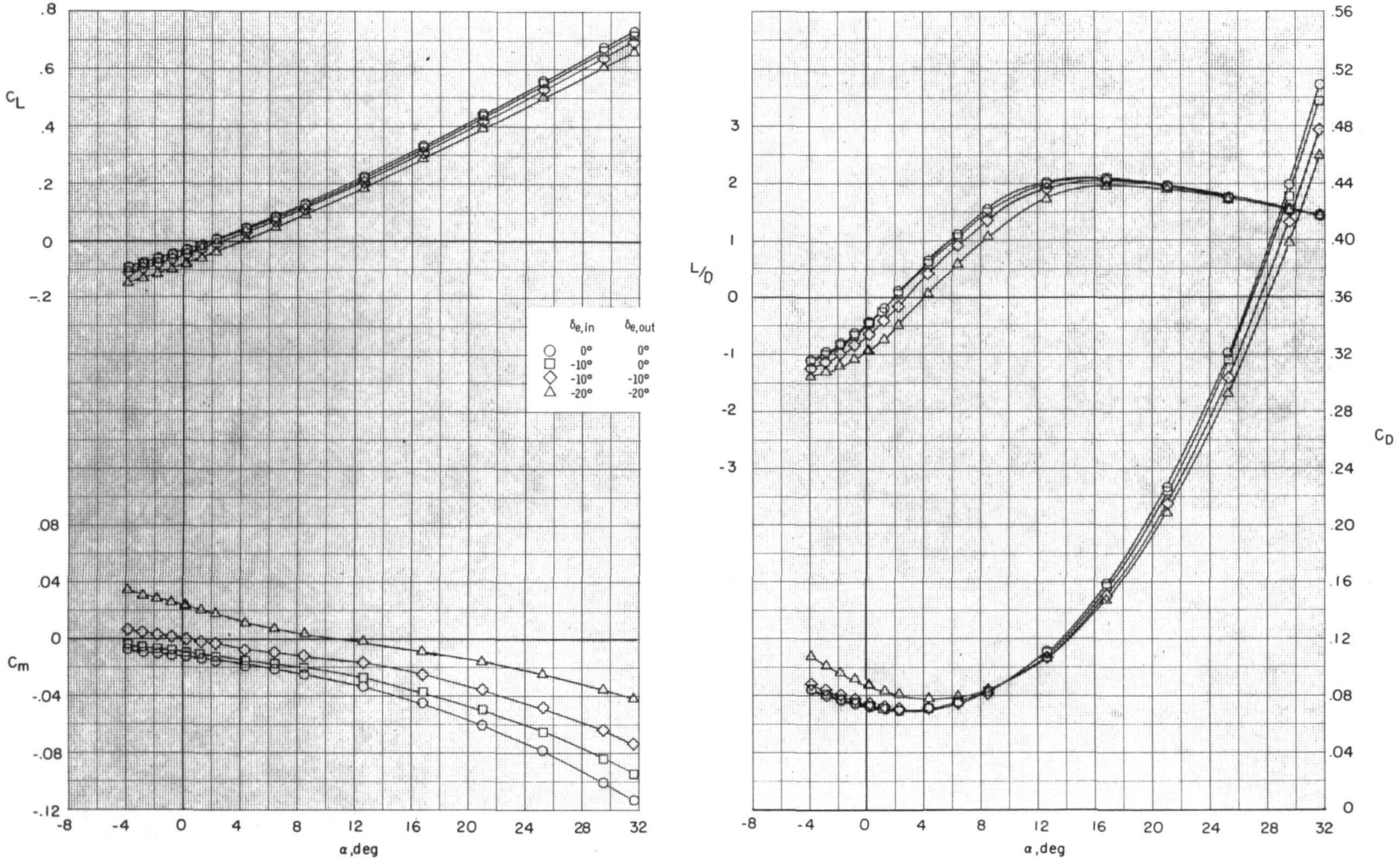

(e) M = 4.63.

Figure 10.- Concluded.

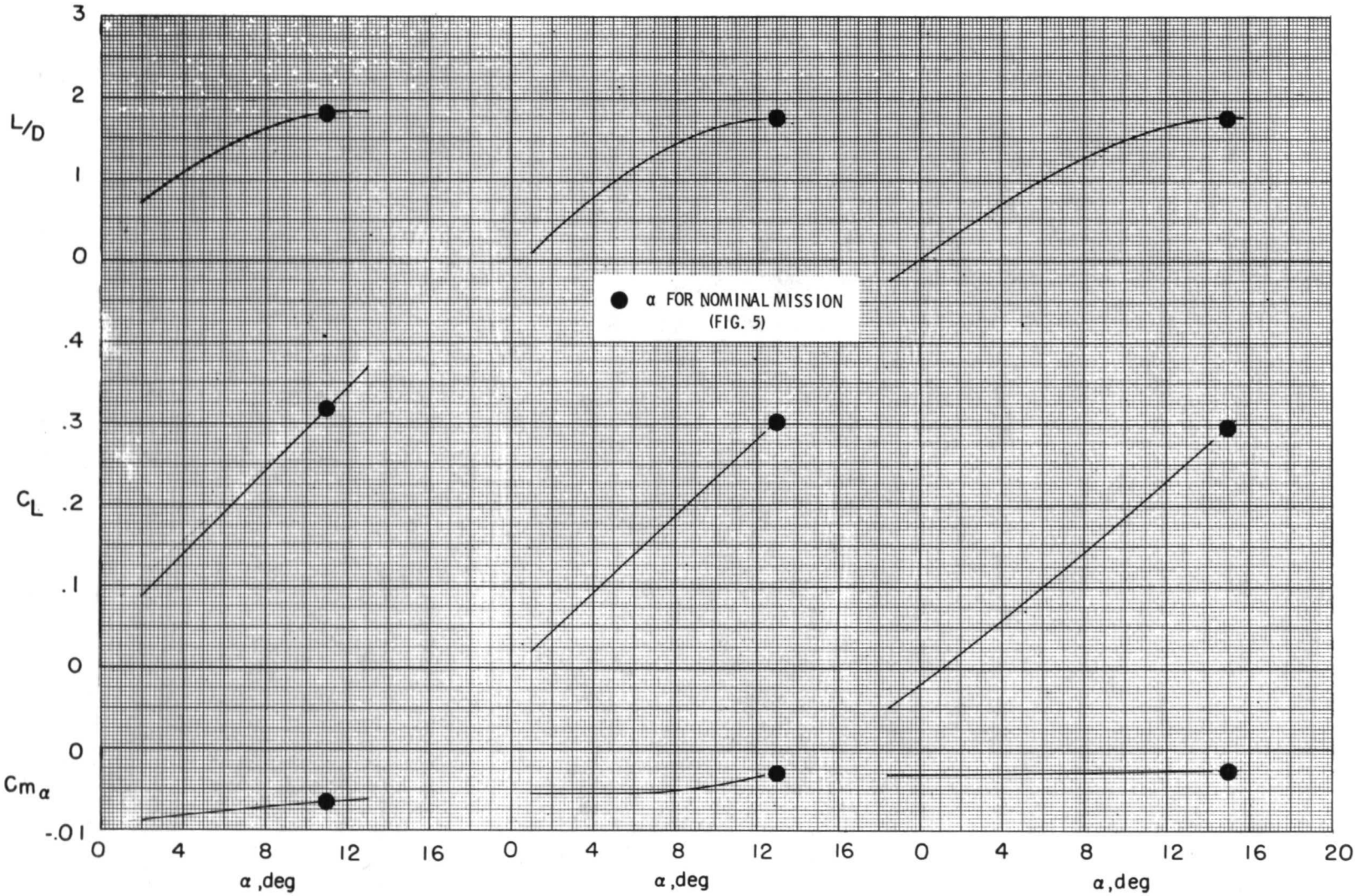

(a) M = 1.90. (b) M = 2.36. (c) M = 2.86.

Figure 11.- Trimmed longitudinal aerodynamic characteristics.

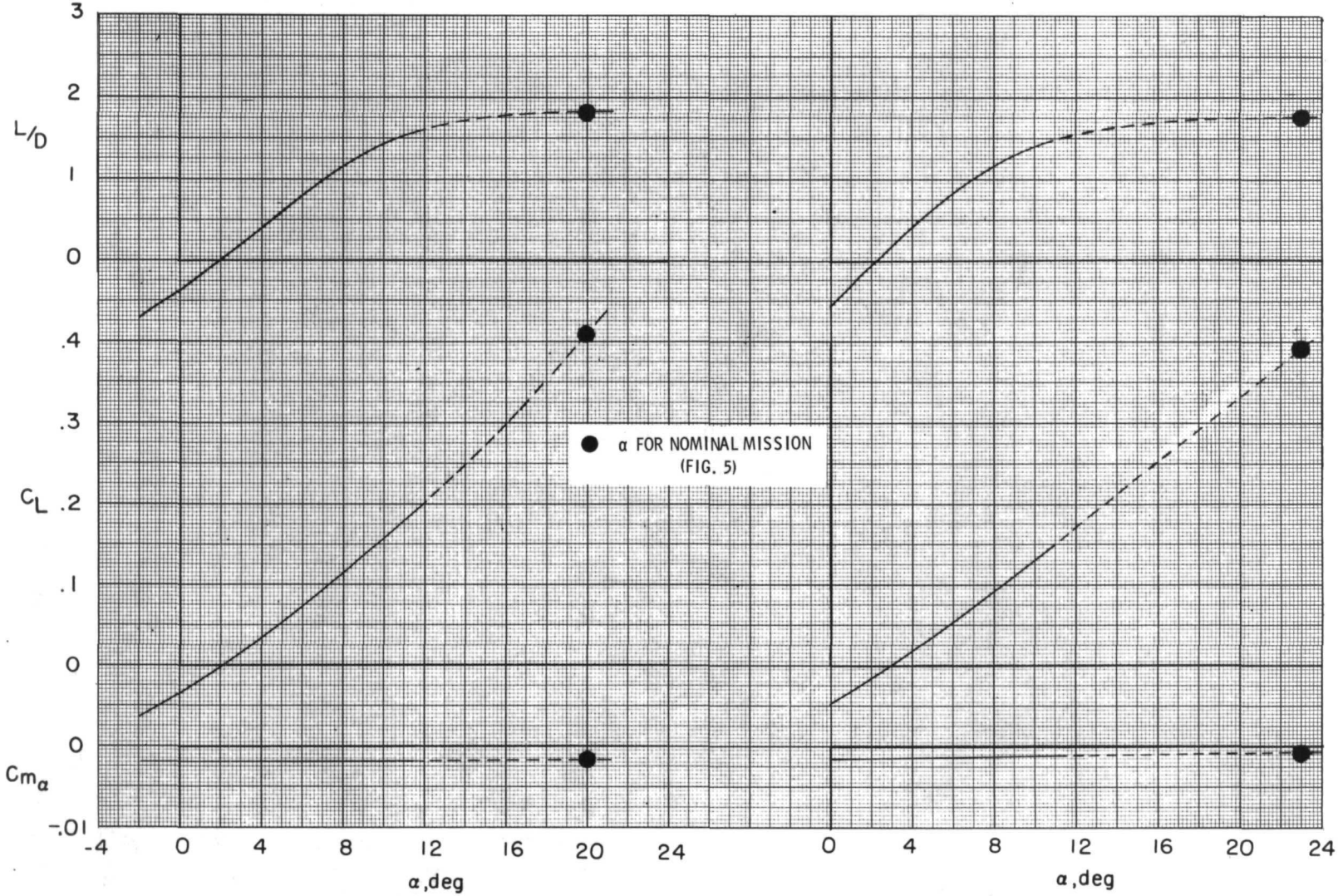

(d) M = 3.96.

(e) M = 4.63.

Figure 11.- Concluded.

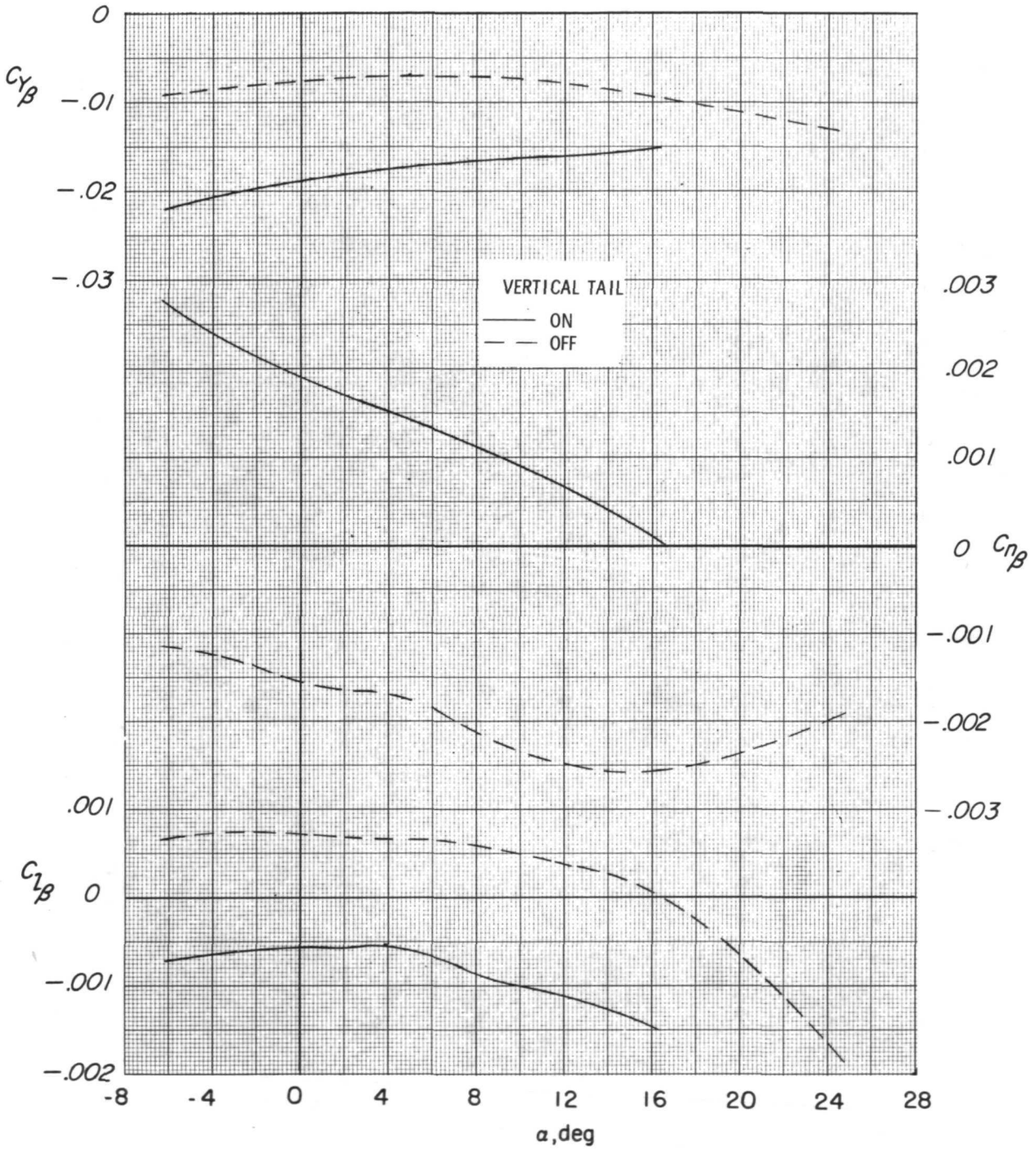

(a) M = 1.90.

Figure 12.- Lateral-directional stability characteristics of the model.

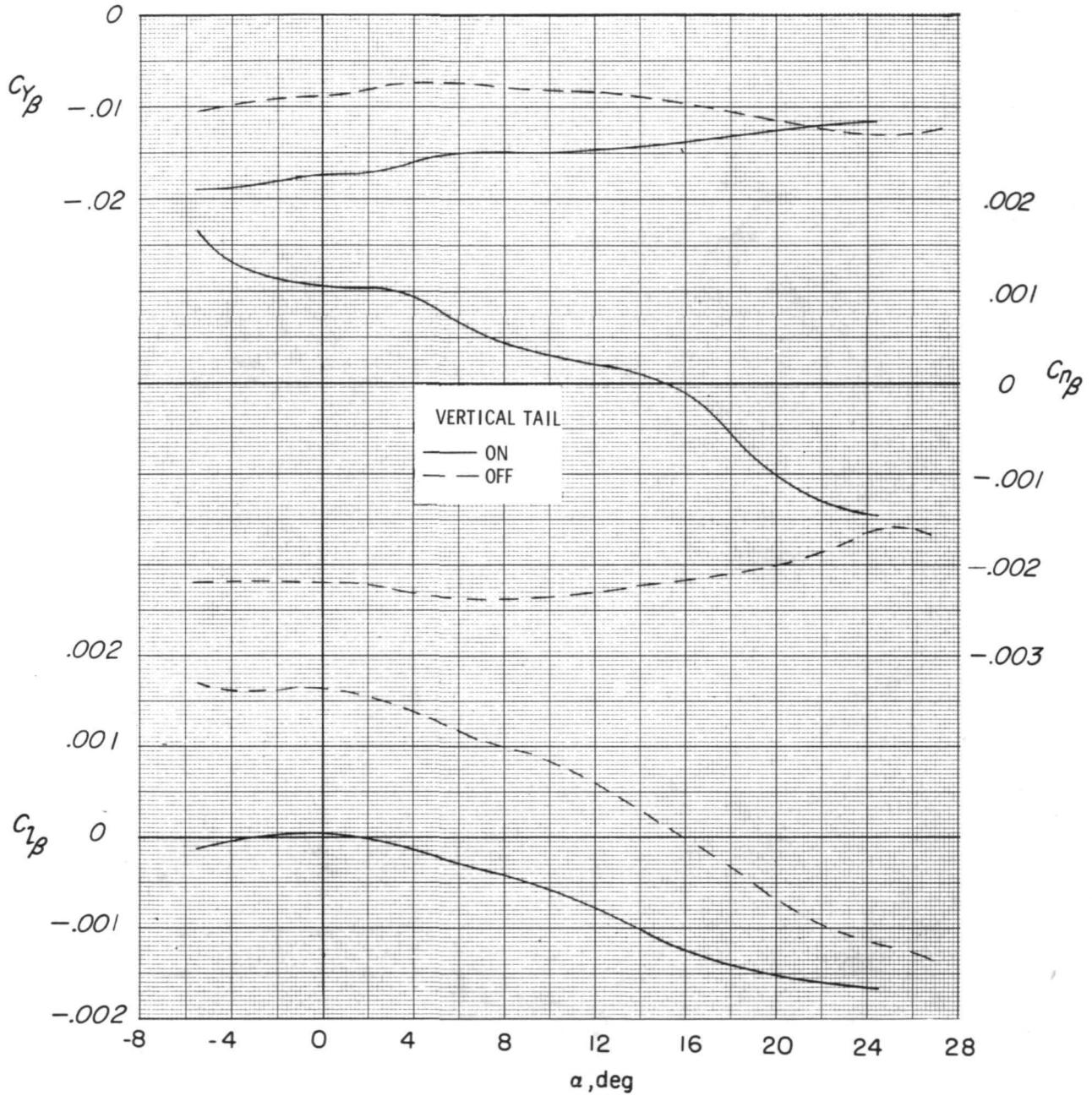

(b) M = 2.36.

Figure 12.- Continued.

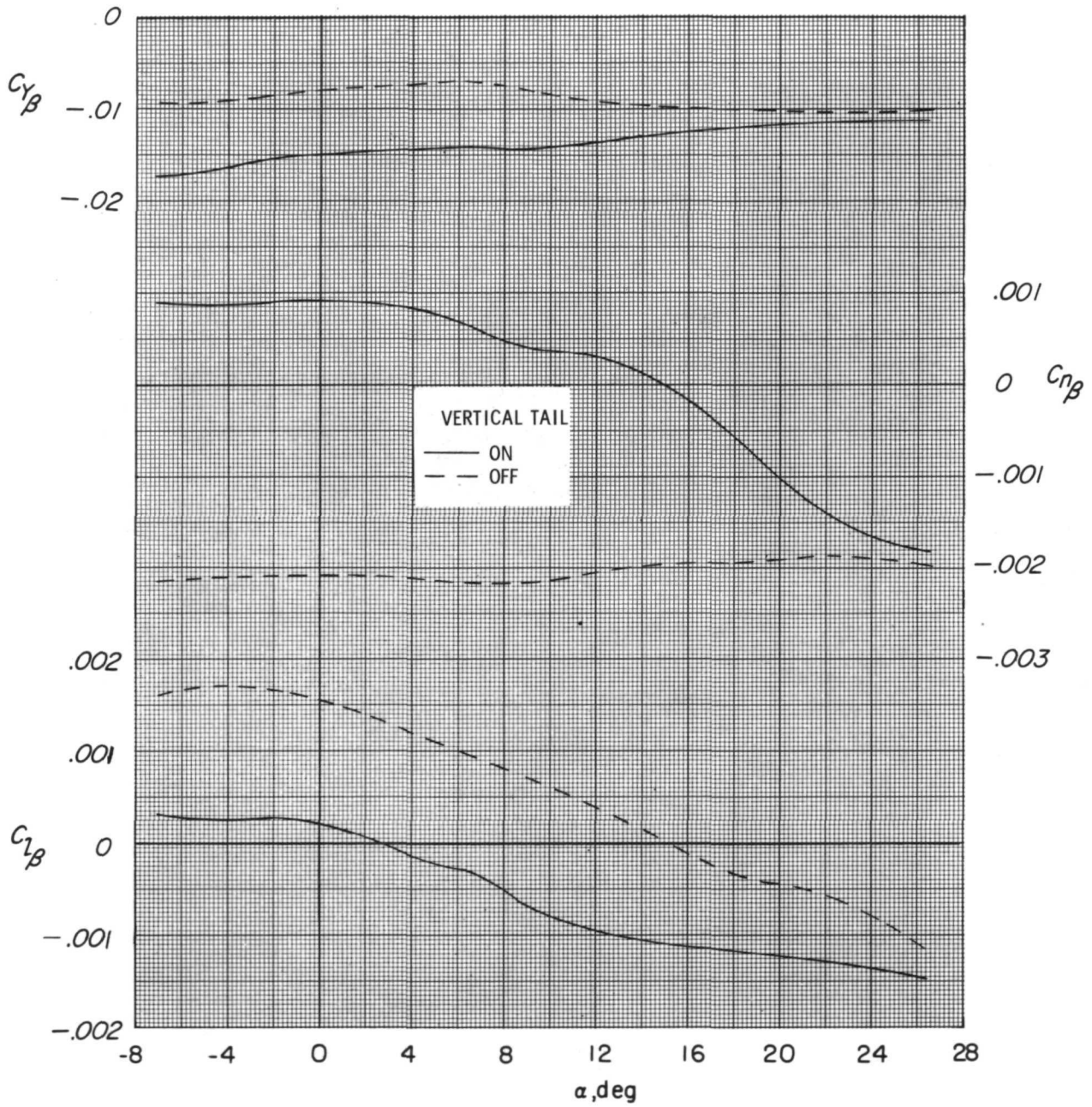

(c) M = 2.86.

Figure 12.- Continued.

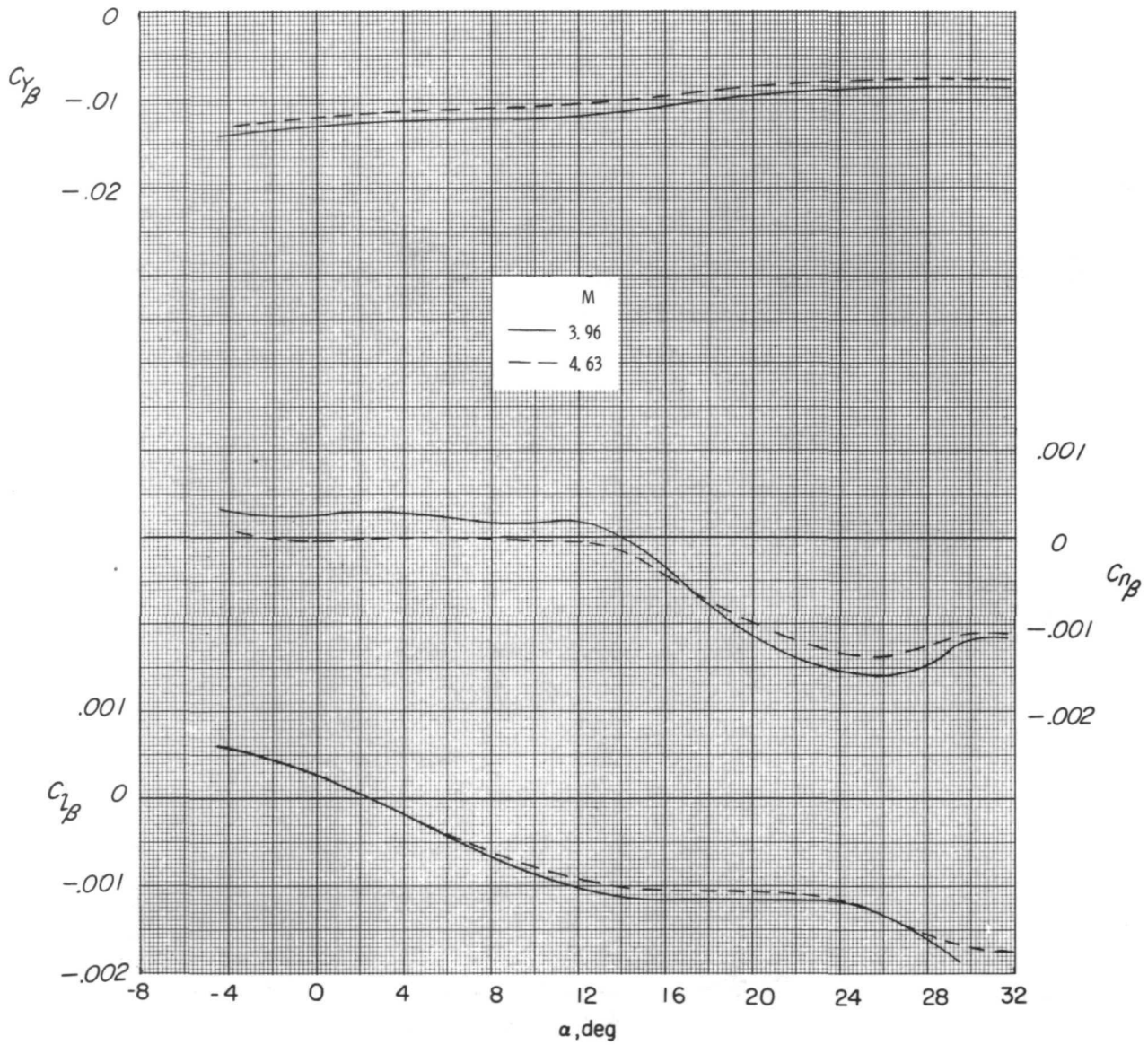

(d) M = 3.96 and 4.63; vertical tail on.

Figure 12.- Concluded.

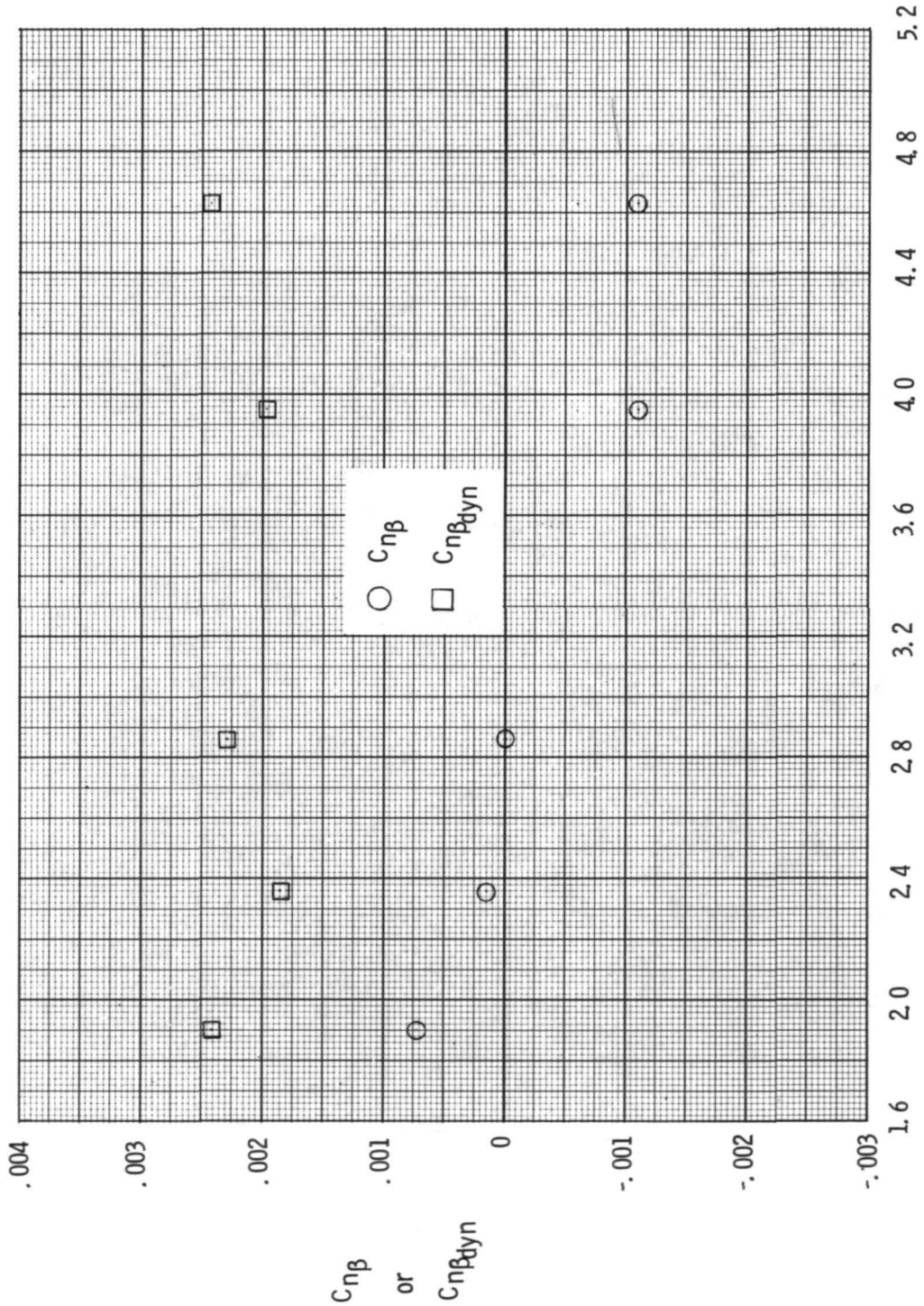

Figure 13.- Directional stability characteristics at nominal mission angles of attack.

NATIONAL AERONAUTICS AND SPACE ADMINISTRATION
WASHINGTON, D.C. 20546

OFFICIAL BUSINESS
PENALTY FOR PRIVATE USE $300

SPECIAL FOURTH-CLASS RATE
BOOK

POSTAGE AND FEES PAID
NATIONAL AERONAUTICS AND
SPACE ADMINISTRATION
451

U.S.MAIL

POSTMASTER: If Undeliverable (Section 158
Postal Manual) Do Not Retur

"The aeronautical and space activities of the United States shall be conducted so as to contribute . . . to the expansion of human knowledge of phenomena in the atmosphere and space. The Administration shall provide for the widest practicable and appropriate dissemination of information concerning its activities and the results thereof."

—NATIONAL AERONAUTICS AND SPACE ACT OF 1958

NASA SCIENTIFIC AND TECHNICAL PUBLICATIONS

TECHNICAL REPORTS: Scientific and technical information considered important, complete, and a lasting contribution to existing knowledge.

TECHNICAL NOTES: Information less broad in scope but nevertheless of importance as a contribution to existing knowledge.

TECHNICAL MEMORANDUMS: Information receiving limited distribution because of preliminary data, security classification, or other reasons. Also includes conference proceedings with either limited or unlimited distribution.

CONTRACTOR REPORTS: Scientific and technical information generated under a NASA contract or grant and considered an important contribution to existing knowledge.

TECHNICAL TRANSLATIONS: Information published in a foreign language considered to merit NASA distribution in English.

SPECIAL PUBLICATIONS: Information derived from or of value to NASA activities. Publications include final reports of major projects, monographs, data compilations, handbooks, sourcebooks, and special bibliographies.

TECHNOLOGY UTILIZATION PUBLICATIONS: Information on technology used by NASA that may be of particular interest in commercial and other non-aerospace applications. Publications include Tech Briefs, Technology Utilization Reports and Technology Surveys.

Details on the availability of these publications may be obtained from:

SCIENTIFIC AND TECHNICAL INFORMATION OFFICE

NATIONAL AERONAUTICS AND SPACE ADMINISTRATION

Washington, D.C. 20546